

Possible *Fermi* Detection of the Accreting Millisecond Pulsar Binary SAX J1808.4–3658

Y. XING, Z. Wang, and V. Jithesh

Shanghai Astronomical Observatory, Chinese Academy of Sciences, 80 Nandan Road, Shanghai 200030, China

wangzx@shao.ac.cn

(Received ; accepted)

Abstract

We report the *Fermi* Large Area Telescope (LAT) detection of a γ -ray source at the position of SAX J1808.4–3658. This transient low-mass X-ray binary contains an accreting millisecond pulsar, which is only seen during its month-long outbursts and likely switches to be rotation powered during its quiescent state. Emission from the γ -ray source can be described by a power law with an exponential cutoff, the characteristic form for pulsar emission. Folding the source’s 2.0–300 GeV photons at the binary orbital period, a weak modulation is seen (with an H-test value of ~ 17). In addition, three sets of archival *XMM-Newton* data for the source field are analyzed, and we find only one X-ray source with 3–4 σ flux variations in the 2σ error circle of the γ -ray source. However based on the X-ray properties, this X-ray source is not likely a background AGN, the major class of *Fermi* sources detected by LAT. These results support the possible association between the γ -ray source and SAX J1808.4–3658 and thus the scenario that the millisecond pulsar is rotation powered in the quiescent state. Considering a source distance of 3.5 kpc for SAX J1808.4–3658, the 0.1–300 GeV luminosity is 5.7×10^{33} erg s $^{-1}$, implying a γ -ray conversion efficiency of 63% for the pulsar in this binary.

Key words: binaries: close — stars: individual (SAX J1808.4–3658) — stars: low-mass — stars: neutron

1. INTRODUCTION

Millisecond radio pulsars (MSPs) are formed from neutron star low-mass X-ray binaries (LMXBs; Bhattacharya & van den Heuvel 1991). The primary neutron star in an LMXB can gain sufficient angular momentum by accreting material from the companion through an accretion disk, and thus be ‘recycled’ to a spin period of milliseconds. The discovery of millisecond X-ray pulsations in the transient LMXB SAX J1808.4–3658 has confirmed the formation scenario from the observational side (Wijnands & van der Klis 1998; Chakrabarty & Morgan 1998). Thus far over a dozen of so-called accreting millisecond X-ray pulsars (AMXPs) have been found (Patruno & Watts 2012). Nearly all of them are in transient systems, and for these transients, X-ray pulsations are seen only during their X-ray outbursts.

Interestingly, it was suggested that several AMXPs actually switch to be rotation powered pulsars during their quiescent states (Burderi et al. 2003; Wang et al. 2013 and references therein), although no direct evidence, such as pulsed radio emission (Burgay et al. 2003), was found over the time. The recent observational identification of the MSP binary J1824–2452I in the globular cluster M28 has firmly confirmed the suggestion (Papitto et al. 2013). The binary was observed to have an X-ray outburst, and during the outburst, the previously known radio MSP in the binary switched to appear like a typical AMXP. This confirmation has thus identified an interesting feature for the evolution from LMXBs to MSP binaries, and we may

suspect that either these systems would probably be at the end of their LMXB phase or it could be a common feature for the quiescent state of transient neutron star LMXBs (e.g., Heinke et al. 2014).

The similar type of feature has also been seen in the recently identified two transitional MSP binaries: J1023+0038 (Archibald et al. 2009) and XSS J12270–4859 (Bassa et al. 2014 and references therein). Extensive observational studies have shown that they can switch between the states of having an accretion disk and being disk free. One particular property in them is that they have sufficiently bright γ -ray emission and are detectable by the *Fermi* Large Area Telescope (LAT; see Tam et al. 2010; Stappers et al. 2014; Takata et al. 2014 for J1023+0038; and see Hill et al. 2011; de Martino et al. 2013; Xing & Wang 2014 for XSS J12270–4859). The emission is variable, stronger in the active accretion state than that in the disk-free state (Stappers et al. 2014; Takata et al. 2014; Xing & Wang 2014). Given the property similarities between the two MSP binaries and AXMP binaries, it is thus highly possible that AMXPs would also have significant γ -ray emission, as they stay in their quiescent state and would be rotation-powered most time. This possibility has been explored by Xing & Wang (2013) by searching for γ -ray emission from four AMXP systems, which include SAX J1808.4–3658. Nearly four year LAT data for the four AMXPs were analyzed, but no γ -ray emission was found. However, given the improved sensitivity of *Fermi* over the last two years (see § 3.1 for details), we re-analyzed the LAT data for them. We found

significant γ -ray emission at the position consistent with that of SAX J1808.4–3658. Here in this paper, we report the results.

2. Observation

LAT is a γ -ray imaging instrument onboard the *Fermi* Gamma-ray Space Telescope. It makes all-sky survey in an energy range from 20 MeV to 300 GeV (Atwood et al. 2009). In our analysis, we selected LAT events from the *Fermi* Pass 7 Reprocessed (P7REP) database inside a $20^\circ \times 20^\circ$ region centered at the optical position of SAX J1808.4–3658, which is R.A.= $18^{\text{h}}08^{\text{m}}27\overset{\text{s}}{.}62$, Decl.= $-36^\circ58'43\overset{\text{s}}{.}3$ (equinox J2000.0) obtained in Hartman et al. (2008). We kept events during the time period from 2008-08-04 15:43:36 (UTC) to 2014-11-10 21:04:57 (UTC) and in the energy range of 100 MeV to 300 GeV. In addition, only events with zenith angle less than 100 deg and during good time intervals were selected. The former prevents the Earth’s limb contamination, and for the latter, the quality of the data was not affected by the spacecraft events.

3. Data Analysis and Results

3.1. Source Identification

We included all sources within 20 deg in the *Fermi* second source catalog (Nolan et al. 2012) centered at the position of SAX J1808.4–3658 (Hartman et al. 2008) to make the source model. The spectral function forms of the sources are provided in the catalog. The spectral parameters of the sources within 5 deg from SAX J1808.4–3658 were set free, and all other parameters of the sources were fixed at their catalog values. A point source at the optical position of SAX J1808.4–3658 was also included in the source model, with its emission modeled by a simple power law. In addition, we used the spectrum model `gll_iem_v05_rev1.fits` and the spectrum file `iso_source_v05.txt` for the Galactic and the extragalactic diffuse emission, respectively, in the source model. The normalizations of the diffuse components were set as free parameters.

Using the LAT science tools software package `v9r33p0`, we performed standard binned likelihood analysis to the LAT data. Events below 200 MeV were rejected because of the relative large uncertainties of the instrument response function of the LAT in the low energy range. Energy ranges of 0.2–300, 0.5–300, 1–300, and 2–300 GeV were tested in the analysis. A source at the optical position was detected with Test Statistic (TS) values of 32, 34, 26, and 31, respectively. The TS value at a specific position, calculated from $\text{TS} = -2\log(L_0/L_1)$ (where L_0 and L_1 are the maximum likelihood values for a model without and with an additional source respectively), is a measurement of the fit improvement for including the source, and is approximately the square of the detection significance of the source (Abdo et al. 2010). Thus the source was best detected in 0.5–300 GeV with a significance of $\simeq 5\sigma$. We extracted the TS maps of a $2^\circ \times 2^\circ$ region centered at the

position of SAX J1808.4–3658 in the four energy ranges, with all sources in the source model considered except the source we found. No catalog sources are within the square region. In Figure 1, the 0.5–300 GeV TS map is shown.

We ran `gtfindsrc` in the LAT software package to determine the position of the source using photons in 0.5–300 GeV, and obtained the best-fit position R.A. = $272^\circ15$, Decl. = $-37^\circ06$ (equinox J2000.0), with 1σ nominal uncertainty of $0^\circ05$. The 2σ error circle is marked in Figure 1 as a dark dashed circle. The optical position of SAX J1808.4–3658 (mark by a dark cross in Figure 1) is $0^\circ08$ from the best-fit position and within the 2σ error circle, suggesting possible association of the γ -ray source with SAX J1808.4–3658. Below we considered the source as the candidate γ -ray counterpart to SAX J1808.4–3658.

In our TS maps, separate excess γ -ray emission at the northwest corner appears (Figure 1). We investigated whether it possibly contaminated our detection of the candidate counterpart. We found that it is consistent with being a point source at a position of R.A. = $271^\circ4$, Decl. = $-36^\circ4$ (equinox J2000.0; 1σ nominal uncertainty is $0^\circ1$). Including this source in our source model, it can be totally removed from the TS maps, and the results of the position and spectrum (see Section 3.2) of the counterpart source did not have significantly differences (consistent within uncertainties).

In addition, since the source position is toward the Galactic center direction ($G_b \simeq -8^\circ1$), we also checked if the uncertainty on the Galactic diffuse emission could produce false detection of the γ -ray source. We manually increased the normalization of the Galactic diffuse component to a value 5σ above the best-fit value, the >0.5 GeV γ -ray emission at the position of SAX J1808.4–3658 was still detected, with $\text{TS} \simeq 32$. We found only when we increased the Galactic diffuse emission by 10% (approximately 77σ above the best-fit value), the >0.5 GeV emission was then detected with $\text{TS} \simeq 9$ (i.e., $\sim 3\sigma$ detection significance).

The γ -ray source was not detected in the previous search using nearly four-year LAT data in >0.2 GeV energy range (Xing & Wang 2013). We re-analyzed the LAT data in the same time interval from 2008-08-04 15:43:36 (UTC) to 2012 July 8 18:59:57 (UTC), and obtained a TS value of $\simeq 25$ at the position of SAX J1808.4–3658, which is much higher than the value of ~ 3 previously reported. Therefore the detection is due to the improved sensitivity of the *Fermi* telescope. The database used in Xing & Wang (2013) is *Fermi* Pass 7, comparing to Pass 7 Reprocessed in this work. The LAT science tools software package and the Instrument Response Functions (IRFs) have also been updated from `v9r27p1` to the current `v9r33p0` and from `P7SOURCE_V6` to `P7REP_SOURCE_V15`, respectively. In addition, the diffuse emission models have also been updated. All these changes have improved the point source detection sensitivity of the *Fermi*/LAT¹.

¹ http://www.slac.stanford.edu/exp/glast/groups/canda/lat_Performance.htm

3.2. Spectral Analysis

Including the γ -ray source in the source model, we performed standard binned likelihood analysis to the LAT data, with emission of this source modeled with an exponentially cutoff power law, which is characteristic of pulsars (Abdo et al. 2013). In addition a simple power law was also used. We used data in >0.2 GeV energy range to obtain a overall description of the γ -ray spectrum of the source. A photon index of $\Gamma = 2.2 \pm 0.1$ with a TS_{pl} value of ~ 32 was obtained for the power-law model, and a photon index of $\Gamma = 1.6 \pm 0.4$ and a cutoff energy of $E_c = 5.5 \pm 3.7$ GeV with a TS_{exp} value of ~ 37 were obtained for the exponentially cutoff power-law model. The low energy cutoff was thus detected with $>2\sigma$ significance (estimated from $\sqrt{TS_{cutoff}}$, where $TS_{cutoff} \simeq TS_{exp} - TS_{pl} \simeq 5$; Abdo et al. 2013). While the significance is low, this result also favors the possible association of the γ -ray source with SAX J1808.4–3658. These spectral results are summarized in Table 1.

We then extracted the γ -ray spectrum for the source, by considering the emission as a point source with a power-law spectrum at the optical position of SAX J1808.4–3658 and performing maximum likelihood analysis to the LAT data in 10 evenly divided energy bands in logarithm from 0.1–300 GeV. The photon index was fixed at 2.2. Only spectral points with $TS \geq 4$ were kept, and the 95% upper limits in other energy bins were derived. The spectrum extracted by this method is less model dependent and provides a more detailed description for the γ -ray emission of the source. The obtained spectrum is shown in Figure 2, and the energy flux values are given in Table 2. It can be seen that the exponentially cutoff power law fits the data better, particularly in low energy ranges where no γ -ray emission was significantly detected.

3.3. Variability Analysis

We performed timing analysis to the LAT data of the SAX J1808.4–3658 region to search for possible γ -ray pulsations. We folded the LAT data according to the X-ray ephemeris given in Hartman et al. (2009). The optical position of SAX J1808.4–3658 was used for the barycentric corrections to photon arrival times, and photons within R_{max} (R_{max} ranges from 0.1 – 1.0 with a step of 0.1) from the position were collected. Different energy ranges (>0.2 , >0.5 , >1 , and >2 GeV) were tested in folding. No pulsation signals were detected, and the H-test values were smaller than 9 (corresponding to $<3\sigma$ detection significance; de Jager et al. 1989).

We folded the LAT data using the orbital parameters given in Hartman et al. (2009). We found that the highest orbital signal was revealed in the >2 GeV energy range using photons within 0.6 from the optical position of SAX J1808.4–3658. The folded light curve, which has an H-test value of ~ 17 (corresponding to $>3\sigma$ detection significance, de Jager et al. 1989), is shown in Figure 3. The phase zero is set at the ascending node of the pulsar in SAX J1808.4–3658.

We also obtained the light curves for the γ -ray source,

with different time intervals (e.g., 30, 100, and 300 days) used. Due to the faintness of the source, no significant flux variations can be determined from the light curves.

3.4. *XMM-Newton* data Analysis

We searched in the SIMBAD Astronomical Database. Most sources identified in the γ -ray source region are not high-energy but star-type objects. There are two other X-ray sources, SAX J1808.5–3703 and SAX J1809.0–3659, previously reported in the region (Wijnands et al. 2002; Campana et al. 2002). While the two sources are 0.02 and 0.11 away from our best-fit position, respectively, there are also other X-ray sources detected in the region but not studied in detail (Campana et al. 2002).

We thus searched and found three archival *XMM-Newton* observations of SAX J1808.4–3658 available. They were carried out on 2001 Mar. 24 (ObsID : 0064940101; exposure 39.5 ks), 2006 Sept. 15 (ObsID : 0400230401; exposure 55.1 ks), and 2007 Mar. 10 (ObsID : 0400230501; exposure 57.8 ks). We analyzed the European Photon Imaging Camera (EPIC) pn and MOS data using the standard tools of the XMM-Newton Science Analysis Software (SAS, version 14.0). For the first observation, pn was used in the timing mode and the data were not included in our analysis. We excluded the high particle flaring background by creating the good time intervals (GTI) based on the count rate cut-off criteria. We extracted the full-field background light curve in the 10–12 keV band and selected the GTI with count rate < 0.8 and $< 0.4 \text{ cts s}^{-1}$ for pn and MOS data respectively. The data were then filtered to the good X-ray events (FLAG == 0) with PATTERN ≤ 4 for pn and PATTERN ≤ 12 for MOS in the 0.3–10 keV energy band.

We then performed the source detection routine (`EDETECT_CHAIN`) on 2007 EPIC-pn data and identified 17 field X-ray sources in the 2σ *Fermi* error circle (radius of 0.1) other than the AMXP, SAXJ 1808.4–3658. Their positions were astrometrically calibrated by correlating the sources detected in the whole pn field with the USNO B1.0 optical catalog (Monet et al. 2003; the SAS task `EPOSCORR` was used). The X-ray field is shown in Figure 4. We obtained the source counts of the 17 sources in both pn and MOS data of the three observations. They were faint with pn count rates of 0.5 – $7.9 \times 10^{-3} \text{ cts s}^{-1}$ and MOS count rates of 0.1 – $2.6 \times 10^{-3} \text{ cts s}^{-1}$. Comparing their count rates in the three observations, we investigated their variability. Out of 17 sources, 16 of them were non-variable ($< 3\sigma$). Only one source, located at R.A.= $18^{\text{h}}08^{\text{m}}54^{\text{s}}.22$, Decl.= $-37^{\circ}06'50''.4$ (equinox J2000.0; 1σ positional uncertainty is $0''.4$), exhibited variability in the count rate at a significance level of $\sim 4\sigma$ and $\sim 3\sigma$ between 2006 and 2007 pn data and 2001 and 2007 MOS data, respectively. However, this source did not show a significant variation ($\sim 2\sigma$) between the 2006 and 2007 MOS data.

We further studied this variable source by fitting its spectra with different models. The count rates were low in the 2001 and 2006 observations, and probably due to this reason, an absorbed power law can provide a good

fit to the spectra. When the column density N_H was set as a free parameter, unphysically large power-law indices of 3–6 were favored. If we fixed $N_H = 1.3 \times 10^{21} \text{ cm}^{-2}$, the Galactic value toward the source direction (Dickey & Lockman 1990), the indices were lowered to 2.9–3.6, and the obtained MOS (absorbed) fluxes were in a range of $1.7\text{--}4.1 \times 10^{-14} \text{ erg cm}^{-2} \text{ s}^{-1}$ and the 2006 pn flux was $1.4^{+0.7}_{-0.5} \times 10^{-14}$. However the 2007 pn spectrum, the most significantly detected (with a count rate of $7.91 \pm 0.71 \times 10^{-3} \text{ cts s}^{-1}$) among the sources and observations, can not be fit with a single model such as a power law (reduced $\chi^2 > 2$; 20 degrees of freedom). We searched the SIMBAD database and USNO B1.0 catalog, no radio or optical counterparts (generally down to 20 mag in R band) were found. Given the properties, we suggest that this source is either a low luminosity X-ray binary or a background galaxy. The power law index values are too high for an AGN (e.g., Ulrich et al. 1997), the largest class among *Fermi* LAT sources (The Fermi-LAT Collaboration 2015).

4. Discussion

Carrying out maximum likelihood analysis of more than 6-year *Fermi* γ -ray data of the source region of SAX J1808.4–3658, we have detected a γ -ray source with the best-fit position consistent with that of AMXP. The source’s γ -ray spectrum can be described by an exponentially cutoff power law. The obtained parameters of $\Gamma = 1.6 \pm 0.4$ and $E_c = 5.5 \pm 3.7 \text{ GeV}$ are within the parameter ranges for pulsars ($0.4 < \Gamma < 2$, $0.4 \text{ GeV} < E_c < 5.9 \text{ GeV}$; see the *Fermi* second pulsar catalog, Abdo et al. 2013), although the uncertainties are large due to low counts of the source. In addition, a possible orbital modulation has also been detected. These results support the association of the γ -ray source with SAX J1808.4–3658.

Observational studies of the transitional MSP binaries (i.e., J1023+0038 and XSS J12270–4859) have shown that γ -ray emission is brighter during their active state when an accretion disk appears (Stappers et al. 2014; Takata et al. 2014; Xing & Wang 2014) than that in the disk-free state, while the radio pulsars are possibly still active but not observable. Very likely in the latter state, the γ -ray emission arises from the magnetosphere of the MSPs (e.g., Takata et al. 2014). In the former state, it has been suggested that either the γ -ray emission is enhanced due to inverse Compton (IC) scattering of a cold pulsar wind off the optical/infrared photons from the accretion disk (Takata et al. 2014), or alternatively self-synchrotron Compton processes at the magnetospheric region of a propelling neutron star is the possible working mechanism for producing γ -ray emission (Papitto et al. 2014). Considering the similarities between the quiescent state of SAX J1808.4–3658 and the active state of the transitional MSP binaries, it is likely that a same emission mechanism also works in the AMXP and thus the observed γ -ray emission is expected.

The orbital modulation from this source was possibly detected. However because of the relative low significance and the unique modulation profile, we can not draw a

certain conclusion. The modulation has two brightness peaks around the inferior conjunction (phase 0.25, when the companion is in front of the neutron star) and the superior conjunction (phase 0.75, when the companion is behind the neutron star) respectively. Such modulation has not been observed in other MSP binaries. Usually there is only one brightness peak, either around the inferior conjunction (see, e.g. PSR J1023+0038 in Bogdanov et al. 2011 and XSS J12270–4859 in Xing & Wang 2014) and possibly due to the occultation of the photon emitting region by the companion, or around the superior conjunction (see, e.g., PSR B1957+20 in Wu et al. 2012, 2FGL J0523.3–2530 in Xing et al. 2014) and possibly due to the viewing angle of the intrabinary interaction region (Wu et al. 2012; Bednarek 2014). Moreover, the orbital signals in these MSP binaries are only seen when accretion disks are not present (Bogdanov et al. 2011; Bogdanov et al. 2014; Xing & Wang 2014). Thus the possible orbital modulation needs further confirmation from different studies. Phase-resolved spectra may help identify the spectral differences and the origin of the modulation. Unfortunately the photon counts from this γ -ray source were too low to allow such analysis.

Considering that the γ -ray emission is from SAX J1808.4–3658, the $>0.1 \text{ GeV}$ γ -ray luminosity of the source is $\sim 5.7 d_{3.5}^2 \times 10^{33} \text{ erg s}^{-1}$ (for the exponentially cutoff power-law model) at the source distance of 3.5 kpc (Galloway & Cumming 2006). The spin-down luminosity \dot{E}_{sd} of SAX J1808.4–3658 is $\sim 9 \times 10^{33} \text{ erg s}^{-1}$ (Hartman et al. 2009), indicating a γ -ray conversion efficiency η_γ of 63%. The efficiency is above the ‘death line’ defined in Xing & Wang (2013) with the characteristic age of $\sim 12 \times 10^9 \text{ yr}$ for SAX J1808.4–3658 (calculated from the pulsar parameters given in Hartman et al. 2009), which supports the suggestion that older MSPs tend to have higher η_γ values.

AGNs are the major class of *Fermi* LAT sources (The Fermi-LAT Collaboration 2015), and they may be identified from their strong variability (e.g., Ulrich et al. 1997; Williamson et al. 2014). We have analyzed three sets of *XMM-Newton* X-ray imaging data of the SAX J1808.4–3658 field, and found 17 faint X-ray sources in the 2σ error circle of the γ -ray source. Among them, only one had $3\text{--}4\sigma$ low flux variations. However, this variable source did not have AGN-like emission, not supporting that it could be a background AGN. We caution that from the X-ray variability study, none of the other 16 sources are likely an AGN, but we can not totally exclude the possibility. In order to identify their nature from spectral properties, deep X-ray observations are needed.

As we write the paper, the *Fermi* third source catalog is released (The Fermi-LAT Collaboration 2015), and we note that the source 3FGL J1808.4–3703 is reported to be detected at the region of SAX J1808.4–3658. The catalog position of 3FGL J1808.4–3703 is R.A. = $272^\circ 12$, Decl. = $-37^\circ 05$ (equinox J2000.0), consistent with the best-fit position we obtained within uncertainties (see Figure 1). Thus our data analysis is confirmed by the catalog results. The catalog source is also identified not to be unassociated

with any known type of objects in the recently available catalogs.

We thank Y. Tanaka and M. Gu for helpful discussion about AGN variability and multiple energy properties. This research made use of the High Performance Computing Resource in the Core Facility for Advanced Research Computing at Shanghai Astronomical Observatory. This research was supported by the Shanghai Natural Science Foundation for Youth (13ZR1464400), the National Natural Science Foundation of China for Youth (11403075), the National Natural Science Foundation of China (11373055), and the Strategic Priority Research Program “The Emergence of Cosmological Structures” of the Chinese Academy of Sciences (Grant No. XDB09000000). Z.W. is a Research Fellow of the One-Hundred-Talents project of Chinese Academy of Sciences. J. V. acknowledges the support by Chinese Academy of Sciences President’s international fellowship initiative (Grant No. 2015PM059).

References

Abdo, A. A., et al. 2010, *ApJS*, 188, 405
 —. 2013, *ApJS*, 208, 17

Archibald, A. M., et al. 2009, *Science*, 324, 1411

Atwood, W. B., et al. 2009, *ApJ*, 697, 1071

Bassa, C. G., et al. 2014, *MNRAS*, 441, 1825

Bednarek, W. 2014, *A&A*, 561, A116

Bhattacharya, D., & van den Heuvel, E. P. J. 1991, *Phys. Rep.*, 203, 1

Bogdanov, S., Archibald, A. M., Hessels, J. W. T., Kaspi, V. M., Lorimer, D., McLaughlin, M. A., Ransom, S. M., & Stairs, I. H. 2011, *ApJ*, 742, 97

Bogdanov, S., Patruno, A., Archibald, A. M., Bassa, C., Hessels, J. W. T., Janssen, G. H., & Stappers, B. W. 2014, *ApJ*, 789, 40

Burderi, L., Di Salvo, T., D’Antona, F., Robba, N. R., & Testa, V. 2003, *A&A*, 404, L43

Burgay, M., Burderi, L., Possenti, A., D’Amico, N., Manchester, R. N., Lyne, A. G., Camilo, F., & Campana, S. 2003, *ApJ*, 589, 902

Campana, S., et al. 2002, *ApJL*, 575, L15

Chakrabarty, D., & Morgan, E. H. 1998, *Nature*, 394, 346

de Jager, O. C., Raubenheimer, B. C., & Swanepoel, J. W. H. 1989, *A&A*, 221, 180

de Martino, D., et al. 2013, *A&A*, 550, A89

Dickey, J. M., & Lockman, F. J. 1990, *ARA&A*, 28, 215

Galloway, D. K., & Cumming, A. 2006, *ApJ*, 652, 559

Hartman, J. M., Patruno, A., Chakrabarty, D., Markwardt, C. B., Morgan, E. H., van der Klis, M., & Wijnands, R. 2009, *ApJ*, 702, 1673

Hartman, J. M., et al. 2008, *ApJ*, 675, 1468

Heinke, C. O., Bahramian, A., Degenaar, N., & Wijnands, R. 2014, ArXiv e-prints

Hill, A. B., et al. 2011, *MNRAS*, 415, 235

Monet, D. G., et al. 2003, *AJ*, 125, 984

Nolan, P. L., et al. 2012, *ApJS*, 199, 31

Papitto, A., Torres, D. F., & Li, J. 2014, *MNRAS*, 438, 2105

Papitto, A., et al. 2013, *Nature*, 501, 517

Patruno, A., & Watts, A. L. 2012, ArXiv e-prints

Stappers, B. W., et al. 2014, *ApJ*, 790, 39

Takata, J., et al. 2014, *ApJ*, 785, 131

Tam, P. H. T., et al. 2010, *ApJL*, 724, L207

The Fermi-LAT Collaboration. 2015, ArXiv e-prints

Ulrich, M.-H., Maraschi, L., & Urry, C. M. 1997, *ARA&A*, 35, 445

Wang, Z., Breton, R. P., Heinke, C. O., Deloye, C. J., & Zhong, J. 2013, *ApJ*, 765, 151

Wijnands, R., Kuiper, L., in ’t Zand, J., Dotani, T., van der Klis, M., & Heise, J. 2002, *ApJ*, 571, 429

Wijnands, R., & van der Klis, M. 1998, *Nature*, 394, 344

Williamson, K. E., et al. 2014, *ApJ*, 789, 135

Wu, E. M. H., Takata, J., Cheng, K. S., Huang, R. H. H., Hui, C. Y., Kong, A. K. H., Tam, P. H. T., & Wu, J. H. K. 2012, *ApJ*, 761, 181

Xing, Y., & Wang, Z. 2013, *ApJ*, 769, 119
 —. 2014, ArXiv e-prints

Xing, Y., Wang, Z., & Ng, C.-Y. 2014, ArXiv e-prints

Table 1. Binned likelihood analysis results for SAX J1808.4–3658.

Spectral model	>0.2 GeV Flux (10^{-9} photon cm $^{-2}$ s $^{-1}$)	Γ	E_c (GeV)	TS
Power law	3.2 ± 0.9	2.2 ± 0.1	...	32
Power law with cutoff	2.4 ± 0.9	1.6 ± 0.4	5.5 ± 3.7	37

Table 2. Flux measurements of SAX J1808.4–3658.

E (GeV)	$F_{\text{low}}/10^{-12}$ (erg cm $^{-2}$ s $^{-1}$)	TS
0.15	1.1	0
0.33	1.7	0
0.74	1.4 ± 0.5	10
1.65	1.0 ± 0.3	10
3.67	0.8 ± 0.3	9
8.17	0.5 ± 0.3	5
18.20	0.5 ± 0.4	4
40.54	0.6	0
90.27	1.8	0
20.10	5.6	0

* Columns 2 and 3 list the energy flux ($E^2 \times dN/dE$) and the TS value in each energy bin, respectively. The fluxes without uncertainties are upper limits.

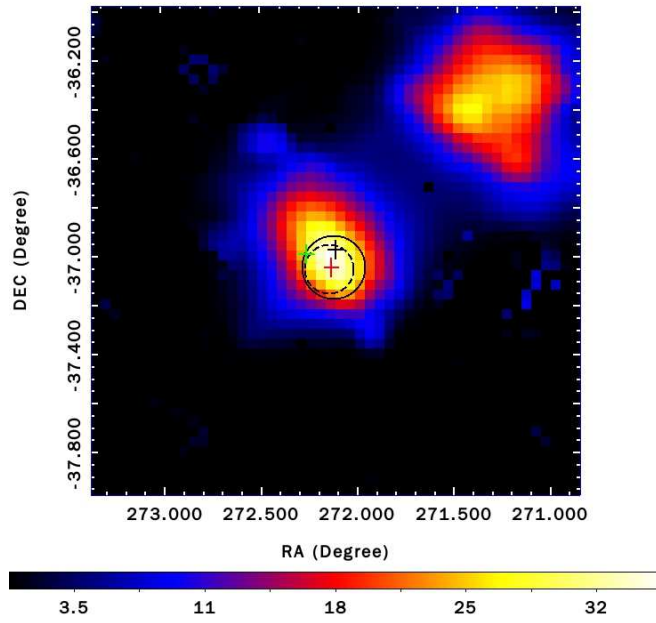


Fig. 1. TS map of a $2^\circ \times 2^\circ$ region, with an image scale of $0.04^\circ \text{ pixel}^{-1}$, centered at the position of SAX J1808.4-3658 in >0.5 GeV energy range. The color bar indicates the TS values. The dark cross marks the optical position of SAX J1808.4-3658. The dark dashed and solid circles are the 2σ error circles of the best-fit position obtained by us and given in the *Fermi* third source catalog for 3FGL J1808.4-3703, respectively.

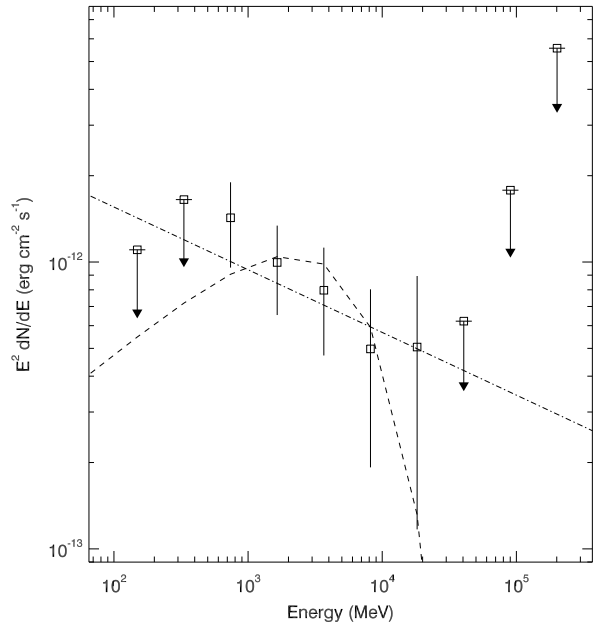


Fig. 2. γ -ray spectrum of SAX J1808.4–3658. The exponentially cutoff power-law and the power-law fits obtained from maximum likelihood analysis are shown as the dashed curve and dot-dashed line, respectively.

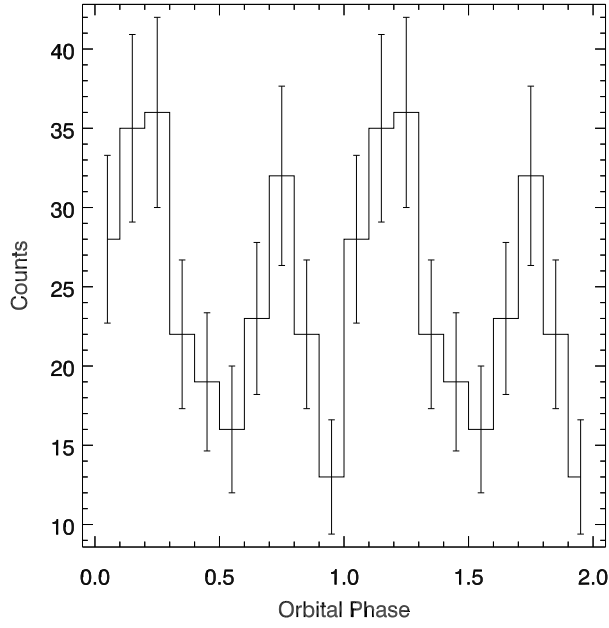


Fig. 3. 2–300 GeV light curve folded with using the X-ray orbital parameters (Hartman et al. 2009). The phase zero is at the ascending node of the MSP in SAX J1808.4–3658.

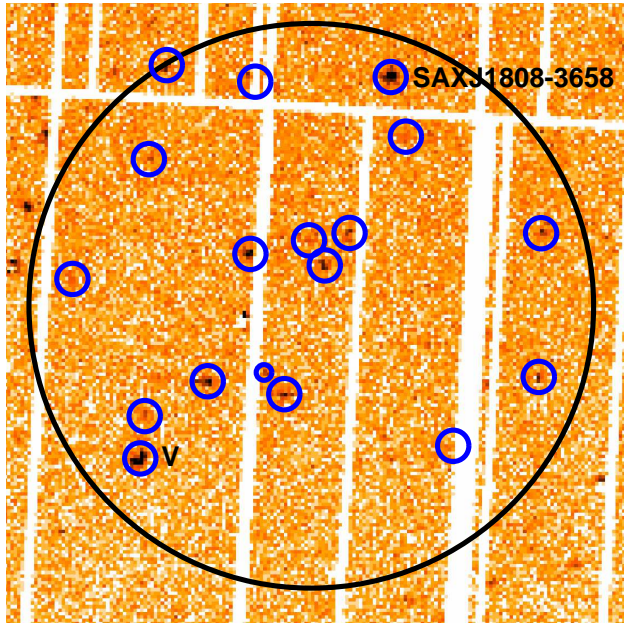


Fig. 4. *XMM-Newton* pn image of the SAX J1808.4–3658 field. The large circle indicates the 2σ error circle of the *Fermi* γ -ray source, in which 17 X-ray sources were detected (marked with small blue circles). The source found with 3–4 σ flux variations is marked with *V*.